Strojniški vestnik - Journal of Mechanical Engineering 70(2024)3-4, 170-180
DOI:10.5545/sv-jme.2023.852
Original Scientific Paper
Received for review: 2023-11-07
Received revised form: 2024-01-09
Accepted for publication: 2024-02-26

Forced Vibration of Time-Varying Elevator Traction System

Jie Sun[1] – Peng Xu[2,3] – Mingli Chen[1] – Jianghong Xue[1,*]
[1]Jinan University, School of Mechanics and Construction Engineering, MOE Key Laboratory of Disaster Forecast and Control in Engineering, China
[2]Qingdao Xinghua Intelligent Equipment Co., China
[3]South China University of Technology, School of Civil Engineering & Transportation, China

This paper proposes a theoretical model for the forced vibration of time-varying elevator traction systems caused by eccentric excitation of the traction machine. Based on the Hamilton principle and a variational principle with variable boundaries, the equations of motion and the complex boundary condition of a time-varying elevator traction system are established. A quantitative formula between the angular velocity of the traction machine, the diameter of the traction wheel, the elevator running distance and the running time is put forward. It is found that when the maximum values of acceleration and deceleration exceed 1.5 m/s², the elevator traction system may undergo resonance.
Keywords: elevator traction system, vibration, time-varying, dynamics, numerical analysis

Highlights
- *The equation of motion and the corresponding boundary condition for forced vibration of a time-varying elevator traction system is derived based on the Hamilton principle and a variational principle with variable boundaries.*
- *A quantitative formula is proposed to describe the relationship between the angular velocity of the traction machine and the diameter of the traction wheel, the running distance, and the running time of the elevator.*
- *It is found that the greater the running acceleration of the elevator, the higher the vibration amplitude and frequency of the elevator traction system.*
- *To prevent the occurrence of resonance, the maximum value of acceleration and deceleration should not exceed 1.5 m/s².*

0 INTRODUCTION

With the continuous emergence of high-rise and super-high-rise buildings, the demand for high-speed elevators continues to grow. Traction elevators are widely used in high-rise buildings due to their advantages, such as low energy consumption and simple structure [1]. Fig. 1 illustrates an elevator traction system.

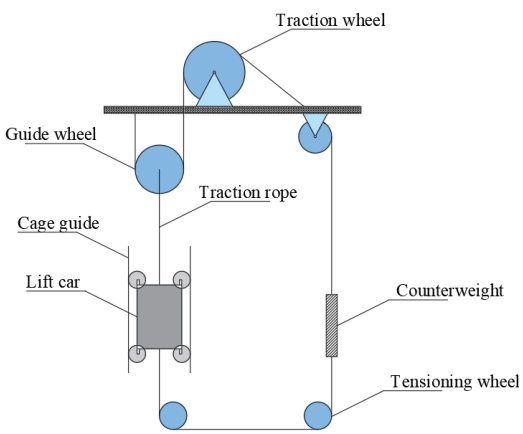

Fig. 1. *Traction system structure*

However, due to the increase in lifting height and operating speed, it is much more difficult to maintain the dynamic stability of the elevator traction system, and the elevators are more sensitive to external interferences and are more prone to undergo abnormal vibrations [2]. These abnormal vibrations may not only affect the working performance of the elevator but also accelerate the wear and fatigue of transmission components, shorten the service life of the elevator, and eventually lead to the occurrence of safety accidents.

Many scholars concentrate on the investigation of the mechanical properties of wire rope. Meng et al. [3] brought forward a theoretical approach to examine the influence of inter-wire contact on the mechanical performances of wire rope strands subjected to tension and torsion loads based on the thin rod and the elastic contact theories. Zhang et al. [4] proposed a theoretical model to investigate the dynamic torsional characteristics of the hoisting rope and its internal spiral components under tension. The variational trend of the twist angle of the wire rope, the lay angle, and the lay length of the spiral strand with the lifting time were discussed. By considering the double-helix structure in multi-strand configuration, Xiang et al. [5] introduced a new method to compute the local deformation of the curvatures and the twist of each wire. It was found that different friction states between adjacent wires can lead to a significantly different

*Corr. Author's Address: Jinan University,GuangDong,China, txue@jnu.edu.cn

distribution of local bending and torsion deformation of double-helix wire. The elastic-plastic deformation of metallic strands and wire ropes under axial–torsional loads were analysed by Xiang et al. [6] based on the thin rod theory of Love and the frictionless assumption of Foti et al. [7], using analytical and 3D finite element methods. For wire ropes with different strand shapes, Stanova et al. [8] developed a 3D solid model by using ABAQUS software and compared the predicted responses for the strands with different shapes and constructions.

The wire ropes of the elevators are flexible with low damping, so they are prone to vibrations [9]. Peng et al. [10] studied the free vibration of elevators in the vertical direction under normal operating conditions theoretically and experimentally. They established a centralized mass discretization model and obtained the theoretical solution. Xu et al. [11] proposed a theoretical model for analysing the tension-torsion coupling vibration of an elevator traction system. According to the Hamiltonian principle, the equation of motion of the elevator traction system with tension-torsional coupling effect is derived and is solved using the Newmark-β method. Based on Bayesian network theory, Zhang et al. [12] put forward a multi-state Bayesian network model for the horizontal vibration of an elevator. Their result can provide quantitative evaluation for the reliability of the multi-state horizontal vibration of the elevator. Much research has been done to investigate the vibrations of the ropes in the elevator system.

Nevertheless, many external interferences, such as the unevenness of the guide rail, the eccentricity of the traction wheel, the airflow disturbance in the lift well and the systematic intrinsic frequency, impact the vibration of the elevator traction system, which would significantly affect riding comfortability and safety. Such a situation is dire for elevators used in ultra-high buildings where the lifting height and the length of wire rope are increased significantly [13] to [15]. By employing the Hamiltonian principle, Bao et al. [16] conducted theoretical analysis for the nonlinear transverse vibration of a flexible hoisting rope with time-varying length and discussed resonance occurring in a passage of the hoisting system due to certain periodic external excitation. Based on the parameters of a typical double-drum Blair multi-rope (BMR) winding plant, Kaczmarczyk [17] proposed a non-linear model to investigate the non-linear dynamic phenomena of a hoisting cable system. The forced vibration of the mine hoisting cables induced by the periodic excitation resulting from the crossover cable motion on the winder drum is analysed. Zhang et al. [18] analysed the sensitivity of random parameters of transverse and horizontal vibration of high-speed elevator lifting systems based on the random perturbation method and analysed the influence of parameters, such as guide length, weight per unit length and bending stiffness, on the dynamic characteristics of a guide. Cao et al. [19] established a trackway-car coupled vibration model via numerical analysis to explore the influence of guide parameters on the lateral vibration of the elevator. The results show that the structural parameters of the guide have a significant influence on the vibration of the elevator system. Zhang et al. [20] studied the horizontal vibration in elevator vertical motion caused by uneven (or non-uniform) elevator guide rails. As the elevator traction systems are installed inside buildings, the swaying of the builds will lead to the vibration of the elevator traction system. Thus, the vibration response of the elevator traction systems is not only dependent on their structural parameters but also affected by the operating environment and building excitation [21] to [23]. Except for the vibration response of the elevator traction system, several researchers focused on the vibration control of the elevator in order to reduce the adverse impact of vibration on the safety performance of the elevator traction system. Nguyen et al. [24] studied the vibration of high-rise elevator ropes under earthquake excitation and verified the effectiveness of the elevator rope vibration suppression controller through numerical simulation. Knezevic et al. [25] proposed a synergistic solution based on the jerk control and the upgrade of the speed controller with a band-stop filter to solve the vibration problem in the process of elevator operation. Zhang et al. [26] developed a model of a cable conveyor system with arbitrarily variable lengths. The Hamiltonian principle was applied to derive the governing equations of motion. The approximate numerical solution of the governing equation was obtained by using the assumed mode method. Based on the precise integration method and Latin hypercube sampling method, Qiu et al. [27] proposed a design parameter optimization method for reducing the horizontal vibration of high-speed elevators.

The above-mentioned literature mainly focused on the free vibration caused by traction acceleration, the transverse vibration due to uneven guide rail, and the vibration control and shock absorption design. However, studies regarding the longitudinal vibration induced by the eccentric excitation of traction wheels are quite limited. In fact, during the operation of the elevator, with the increase of the angular speed of the traction wheel, the acceleration of the traction system

will increase, leading to the improvement of the eccentric excitation. When the angular speed of the traction wheel reaches a certain value, the frequency of the longitudinal vibration generated by the eccentric excitation of the traction wheel will be close to the natural frequency of the system itself, resulting in the occurrence of resonance phenomenon, which greatly affects the safety of the elevator operation. Such a phenomenon has not been discussed in the existing literature. In this paper, the longitudinal vibration of elevator traction systems with and without external excitation is investigated by considering the time-varying characteristics of elevator traction systems. An analytical model is employed to analyse the vibration performance of the elevator traction system subjected to the eccentric excitation of traction wheels. The relationship between the acceleration of the elevator traction system and the angular velocity of the traction wheel is proposed, and the influence of elevator operating acceleration on the resonance of the elevator is discussed. A safe range of acceleration is proposed in order to prevent the resonance of the elevator. The results from this study provide a reference for improving elevator safety and seismic design.

1 METHOD

1.1 Time-Varying Elevator Traction System

An elevator traction system mainly consists of a traction wheel, a lifting car, and a wire rope. The wire rope is simplified as a variable-length cord moving along the axis; the lifting car is simplified as a rigid body suspended at the lower end of the cord with a mass of m. Fig. 2 is an analytical model for the longitudinal vibration of time-varying elevator traction systems. A coordinate system is established with the origin located at the tangent point of the wire rope and pulley, and the positive direction is chosen as the downward direction, as shown in Fig. 2. During the movement, the longitudinal displacement at a spatial position x(t) on the wire rope is described as u(x(t), t). The elevator traction system has an acceleration a(t) and an axial velocity v(t) corresponding to a wire rope length x(t). The analytical model for the longitudinal vibration of a time-varying elevator traction system is based on the following assumptions. The elevator traction system only undergoes longitudinal vibration. During operation, the wire rope is always in tension and complies with Hooke's Law, and its elastic modulus remains constant along the whole length.

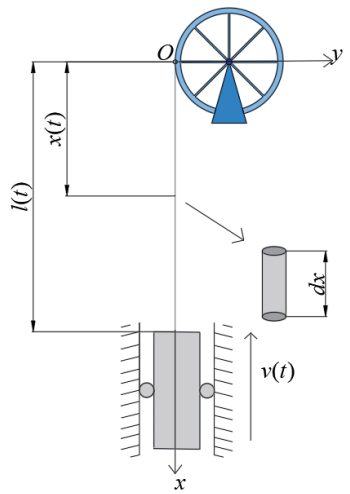

Fig. 2. *Time-varying longitudinal vibration model of elevator traction system*

According to the finite deformation theory of continuum mechanics, the displacement of the wire rope at time t at a spatial position $x(t)$ is

$$l = \left[x(t) + u\left(x(t), t\right) \right]. \tag{1}$$

The total velocity V at the spatial position $x(t)$ of the wire rope is the summation of the axial velocity $v(t)$ of the elevator and the vibration velocity at $x(t)$ and is expressed as:

$$V = \frac{dl}{dt} = \left[v(t) + \left(u_t(t) + v \cdot u_x(t) \right) \right]. \tag{2}$$

where the subscript of x or t denoted the partial differentiation with respect to x or t.

The kinetic energy of the elevator traction system is expressed as follows.

$$E_k = 0.5 m v_c^2 \Big|_{x=l(t)} + 0.5\rho \int_0^{l(t)} V^2 dx, \tag{3}$$

where the first term is the kinetic energy of the lifting car, and the second term is the kinetic energy of the wire rope.

Since the lifting car is considered to be a rigid body, the elastic strain energy of the elevator traction system is that of the wire rope, which is formulated as follows:

$$E_s = \int_0^{l(t)} (P u_x + 0.5 E A u_x^2) dx, \tag{4}$$

where E and A are Young's modulus and the nominal cross-section area of the wire rope, respectively. P is the quasi-static tension measured at the spatial position $x(t)$ on the wire rope and is expressed by:

$$P=\left[m+\rho\left(l\left(t\right)-x\right)\right]g. \tag{5}$$

In Eq. (4), the first term in the bracket denotes the static strain energy, and the second term represents the dynamic strain energy. The gravitational potential energy of the elevator traction system is:

$$E_g=-\int_0^{l(t)}\rho gudx-mgu\big|_{x=l(t)}. \tag{6}$$

1.2 Dynamic Model Without External Interference

The elevator starts to run when an acceleration a(t) is provided by a lift machine. Furthermore, vibration is also generated in the elevator traction system. According to the Hamiltonian principle, the movement trajectory of the elevator in any time interval makes the time integral of the total energy stationary, that is:

$$I=\int_{t_1}^{t_2}\left[\delta E_k-\delta E_s-\delta E_g\right]dt=0. \tag{7}$$

The boundary conditions of the elevator traction are:

$$\delta u\left(0,t\right)=\delta u\left(x,t_1\right)=\delta u\left(x,t_2\right)=0,$$
$$u\left(0,t\right)=0. \tag{8}$$

Using integral by parts with a variable upper boundary, the expression of δE_k, δE_g and δE_s are further reformed as follows:

$$\begin{aligned}\int_{t_1}^{t_2}\delta E_k dt=&-\int_{t_1}^{t_2}\left\{m\frac{\partial}{\partial t}\left(v+u_t+vu_x\right)\right.\\&\left.+m\frac{\partial}{\partial x}\left[v\left(v+u_t+vu_x\right)\right]\right\}\delta u\big|_{x=l(t)}dt\\&-\int_{t_1}^{t_2}\left\{\rho\int_0^{l(t)}\frac{\partial}{\partial t}\left(v+u_t+vu_x\right)\delta u dx\right.\\&\left.-\int_0^{l(t)}\left[\rho v\int_0^{l(t)}\frac{\partial}{\partial x}\left(v+u_t+vu_x\right)\right]\right\}dt,\end{aligned} \tag{9}$$

$$\int_{t_1}^{t_2}\delta E_g dt=-\int_{t_1}^{t_2}\left(mgu\big|_{x=l(t)}+\int_0^{l(t)}\rho gudx\right)\delta dt, \tag{10}$$

$$\begin{aligned}\int_{t_1}^{t_2}\delta E_s dt=&\int_{t_1}^{t_2}\left[\left(P\delta u+EAu_x\delta u\right)\big|_{x=l(t)}\right.\\&\left.-\int_0^{l(t)}\left(P_x\delta u-EAu_{xx}\right)\delta u dx\right]dt.\end{aligned} \tag{11}$$

Substitute Eqs. (9) to (11) into Eq. (7). By applying Leibniz's formula and considering the arbitrary property of δu, the following equations are derived:

$$\rho\left(u_{tt}+2vu_{xt}+au_x+v^2u_{xx}+a\right)=EAu_{xx},$$
$$0<x<l\left(t\right), \tag{12}$$

$$m\left(u_{tt}+2vu_{xt}+au_x+v^2u_{xx}+a\right)+EAu_x=0,\ x=l\left(t\right). \tag{13}$$

Eq. (12) is the equation of motion for the longitudinal vibration of the time-varying elevator traction system and Eq. (13) is the corresponding boundary conditions of the elevator traction system.

1.3 Dynamic Model with External Interference

As one of the external interferences, the eccentricity of the traction wheel will produce an eccentric force during the operation of the elevator, which leads to the force vibration of the elevator traction system. Due to the limitations of the manufacturing technology, errors from the manufacture and installation cause a deviation of the central axis of the traction wheel from the rotating axis, resulting in the eccentricity of the traction wheel. The boundary condition in this situation is formulated as:

$$u\left(0,t\right)=e,\quad u\left(l,t\right)=0, \tag{14}$$

where e is the eccentric excitation displacement dependent on time. Note that the boundary conditions in Eq. (14) are nonhomogeneous. To solve the governing Eq. (12) by satisfying the boundary conditions in Eq. (14), the displacement function $u\left(x,t\right)$ is decomposed into two parts:

$$u\left(x,t\right)=u_1\left(x,t\right)+u_2\left(x,t\right), \tag{15}$$

where $u_1\left(x,t\right)$ satisfies the homogeneous boundary conditions, and $u_2\left(x,t\right)$ satisfies the nonhomogeneous boundary conditions in Eq. (14). Since this paper studies the vibration of the time-varying elevator traction system under the influence of periodic forces, the expression $u_2\left(x,t\right)$ is obtained according to the stress-strain relationship as follows:

$$u_2\left(x,t\right)=e-\frac{e}{l}x. \tag{16}$$

Substituting Eq. (16) into (15) and then the acquired Eqs. (12) and (13), the equation of motion and the corresponding boundary condition for the forced longitudinal vibration of the time-varying elevator traction system are obtained as follows:

$$\begin{aligned}\mathfrak{D}\left(u(x,t)\right)=&\rho\left(u_{1,tt}+2vu_{1,xt}+au_{1,x}+v^2u_{1,xx}+a\right)\\&-EAu_{1,xx}-\rho\left\{2v\left(\frac{le_t-ve}{l^2}\right)+\frac{ae}{l}\right.\\&\left.+\left[\frac{e_{tt}}{l}-\frac{ae}{l^2}-\frac{2ve_t}{l^2}+\frac{2v^2e}{l^3}\right]x\right\}=0,\\&0<x<l\left(t\right),\end{aligned} \tag{17}$$

$$\mathfrak{B}\left(u(x,t)\right)=m\left(u_{1,tt}+2vu_{1,xt}+au_{1,x}+v^2u_{1,xx}+a\right)+EAu_{1,x}-\frac{EAe}{l}+m\left\{2v\frac{ve-le_t}{l^2}-\frac{ae}{l}+\left[-\frac{e_{tt}}{l}+\frac{2ve_t}{l^2}+\frac{ae}{l^2}-\frac{2v^2e}{l^3}\right]x\right\}=0,\quad x=l(t). \tag{18}$$

1.4 Discretization Process

Since the equation of motion, Eq. (17), for the longitudinal vibration of the time-varying elevator system is a complex partial differential equation with infinite degrees of freedom and time-varying parameters, it is almost impossible to obtain accurate solutions. In this paper, the Galerkin method is used to discretize the equation of motion so that the equation of motion is converted into a set of ordinary differential equations. Following this work, the Newmark-β method is applied to obtain the numerical solution. The Newmark-β method is a numerical calculation method that linearizes and averages the generalized acceleration in the equation of motion for a dynamic problem. It is one of the most commonly used numerical methods in finite element analysis for dynamic problems and can ensure stable numerical solutions **[28]**. The solution of u1 is assumed in the form:

$$u_1(x,t)=\sum_{i=1}^{n}\varphi_i(x)\,p_i(t), \tag{19}$$

where $p_i(t)$ is the generalized coordinate, and n is the number of included modulus, $\varphi_i(x)$ is the trial function. Since the wire rope is considered as a cantilever beam, the trial function $\varphi_i(x)$ is taken as the following form:

$$\varphi_i(x)=\sqrt{2}\sin\left(\frac{2i-1}{2l}\pi x\right). \tag{20}$$

Although Eq. (20) satisfies the boundary condition in Eq. (8) at $x = 0$, it cannot satisfy the boundary condition in Eq. (18) at $x = l(t)$. To eliminate the residuals generated by the trial function in the domain of x and at the boundary of x, the method of weighted residuals is adopted, which requires the total residual of the trial function in the domain of x and that at the boundary of x vanish:

$$\int_0^{l(t)}\mathfrak{D}_j(u,\varphi)\varphi_i(x)dx+\mathfrak{B}_j(u,\varphi)\varphi_i(x)|_{x=l(t)}=0,\quad (i,j=1,2,\cdots,n). \tag{21}$$

For the convenience of analysis, a new variable $\xi = x/l(t)$ is defined to normalize the variable x, and the time-varying domain $[0, l(t)]$ related to x is transformed into a fixed domain [0, 1] of ξ. Replace $x = \xi\, l(t)$. After some calculus calculation, the equations of motion are transformed into the following form of the matrix:

$$M\ddot{p}+C\dot{p}+Kp=F, \tag{22}$$

where

$$\begin{aligned}
M_{ji}&=\rho\delta_{ij}+\frac{m}{l(t)}\phi_i(1)\phi_j(1),\\
C_{ji}&=\frac{2\rho v(t)}{l(t)}\int_0^1(1-\xi)\phi_i'(\xi)\phi_j(\xi)d\xi,\\
K_{ji}&=\frac{\rho v^2(t)}{l^2(t)}\int_0^1(1-\xi)^2\varphi_i''(\xi)\varphi_j(\xi)d\xi\\
&\quad-\frac{EA}{l^2}\int_0^1\varphi_i''(\xi)\varphi_j(\xi)d\xi\\
&\quad+\frac{a\rho}{l}\int_0^1(1-\xi)\varphi_i'(\xi)\varphi_j(\xi)d\xi\\
&\quad-\frac{2v^2\rho}{l^2}\int_0^1(1-\xi)\varphi_i'(\xi)\varphi_j(\xi)d\xi+\frac{EA}{l^2}\varphi_i'(1)\varphi_j(1)\\
F_j&=-\rho\int_0^1\left[2v\left(e_t-\frac{ve}{l}\right)+ae+\xi\left(e_{tt}l-ae-2ve_t+\frac{2v^2e}{l}\right)\right]\varphi_j(\xi)d\xi-\rho a\int_0^1\varphi_j(\xi)d\square\\
&\quad-\frac{ma}{l}\varphi_j(1)-\left(me_{tt}+\frac{EAe}{l}\right)\varphi_j(1),
\end{aligned} \tag{23}$$

and δ_{ij} is the delta function. Eqs. (22) and (23) are solved by using Newmark-β method. Fig. 3 is a flow chart to solve Eqs. (22) and (23) by developing a MATLAB program.

2 MODELLING OF THE RUNNING STATUS OF THE ELEVATOR TRACTION SYSTEM

A complete running cycle of the elevator includes at least seven stages: acceleration increasing $(0, t_1)$, uniform acceleration (t_1, t_2), the acceleration decreasing to zero (t_2, t_3), uniform motion (t_3, t_4), deceleration increasing to the maximum (t_4, t_5), uniform deceleration (t_5, t_6), and deceleration decreasing to zero (t_6, t_7). The hoisting jerk $j_i(t)$ (the change of the acceleration per unit time) of the elevator at Stage I is taken as a quadratic function of time as follows:

$$j_i(t)=60\eta_0^i(t-t_{i-1})^2+24\eta_1^i(t-t_{i-1})+6\eta_2^i. \tag{24}$$

Assuming that the maximum acceleration, the maximum speed, and the maximum jerk are a_m, v_m, j_m, respectively, the jerk $j_i(t)$, hoisting acceleration

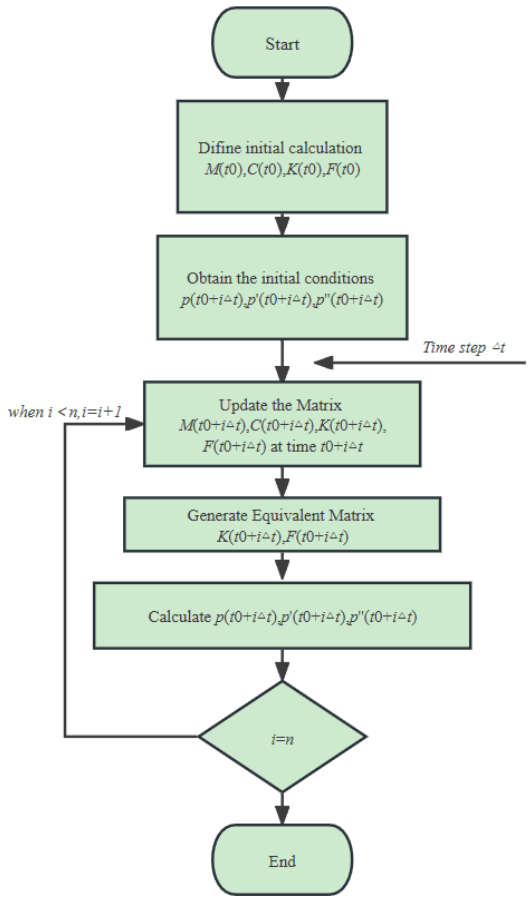

Fig. 3. *A flow chart to solve Eqs. (22) and (23)*

$a_i(t)$, the hoisting speed $v_i(t)$ and the length $l_i(t)$ of the elevator at each stage are determined by integrating sequential and applying the continuity conditions. Fig. 4 shows typical running curves of an elevator when it goes up and down.

3 NUMERICAL RESULTS AND DISCUSSION

As an example, the typical parameters of the elevator traction system in a high-rise elevator are ρ = 0.575 kg/m, m = 1000 kg, $EA = 7.02\times10^7$ N. The length of the wire rope is l_0 = 140 m.

According to the Newmark method, the iteration equation for solving Eq. (22) in the given time domain is derived as follows:

$$\widehat{K}_{t+\Delta t}\, p_{t+\Delta t} = \widehat{F}_{t+\Delta t},$$

$$\dot{p}_{t+\Delta t} = \frac{\gamma}{\beta\Delta t}\left(p_{t+\Delta t} - p_t\right) + \left(1-\frac{\gamma}{\beta}\right)\dot{p}_t + \left(1-\frac{\gamma}{2\beta}\right)\ddot{p}_t\Delta t,$$

$$\ddot{p}_{t+\Delta t} = \frac{1}{\beta\Delta t^2}\left(p_{t+\Delta t} - p_t\right) - \frac{1}{\beta\Delta t}\dot{p}_t - \left(\frac{1}{2\beta}-1\right)\ddot{p}_t, \qquad (25)$$

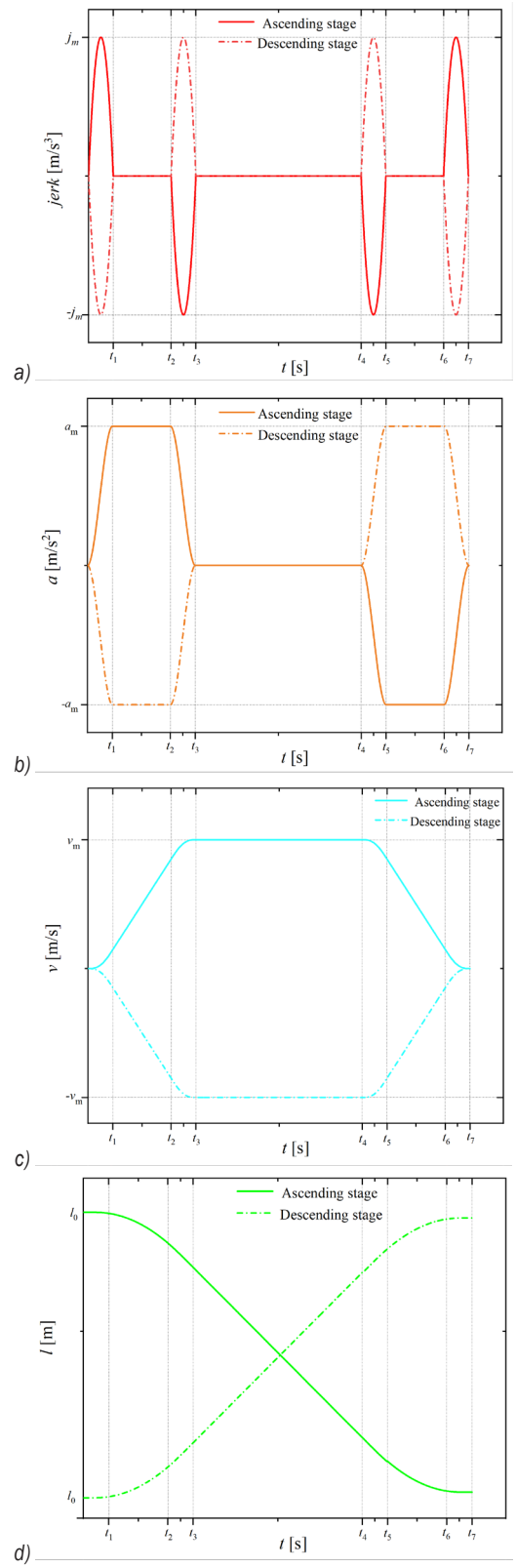

Fig. 4. *Typical running curves of an elevator: a) Increase of acceleration, b) acceleration of elevator, c) velocity of the elevator, d) length of wire rope*

where

$$\widehat{K} = K_{t+\Delta t} + \frac{1}{\beta \Delta t^2} M + \frac{\gamma}{\beta \Delta t} C,$$

$$\widehat{F} = F_{t+\Delta t} + M\left[\frac{1}{\beta \Delta t^2} p_t + \frac{1}{\beta \Delta t} \dot{p}_t + \left(\frac{1}{2\beta} - 1\right) \ddot{p}_t\right] + C\left[\frac{\gamma}{\beta \Delta t} p_t + \left(\frac{\gamma}{\beta} - 1\right) \dot{p}_t + \left(\frac{\gamma}{2\beta} - 1\right) \ddot{p}_t \Delta t\right], \quad (26)$$

γ and β are the calculation parameters from the algorithm of the Newmark-β method. In this paper, $\gamma = 1/2$ and $\beta = 1/4$.

At time $t = 0$, the elevator traction system is stationary. Thus, the initial values of the generalized coordinate and its velocity are zero, i.e., $[p_0] = 0$ and $\begin{bmatrix}\dot{p}_0 \\ \ddot{p}_0\end{bmatrix} = 0$. As to the initial value of the acceleration of $\begin{bmatrix}\dot{p}_0 \\ \ddot{p}_0\end{bmatrix}$, it is obtained from Eq. (22) with the known values of $[p_0]$ and $[\dot{p}_0]$. In the following of this section, the influence of the running direction, the acceleration, and the mass of the lifting car on the vibration performance of the elevator traction system is under investigation.

3.1 Vibration Without the Eccentric Excitation

Table 1 lists the time interval of the seven stages in a complete running cycle of the elevator traction system. Fig. 5 plots the time history for the longitudinal vibration of the elevator traction system without the eccentric excitation when $v_m = 5$ m/s and $a_m = 1$ m/s².

It can be seen from Fig. 5 that regardless of whether the elevator is in the ascending or descending stages, aperiodic displacement occurs during the starting and braking stages. These aperiodic displacements are attributed to the inertial force from the acceleration or deceleration, indicating that the elevator deviates from the initial equilibrium position. Another observation from Fig. 5 is that the vibration amplitude and frequency of the elevator traction system decrease during the ascending stage and increase during the descending stage. The reason for such response is that the length of the steel wire rope is reduced during the ascending process, which causes the increasing of the stiffness of the elevator traction system, as a result of that, the amplitude and frequency of the longitudinal vibration decreases. The situation is reversed during the descending process.

Table 1. *Time interval of seven stages in a complete running cycle of the elevator traction system [s]*

t_1	t_2	t_3	t_4	t_5	t_6	t_7
1.5	5	6.5	16.5	18	21.5	23

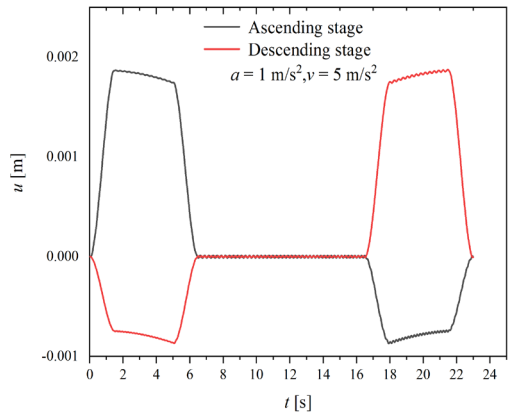

Fig. 5. *The time history of longitudinal vibration of the elevator traction system without external interference*

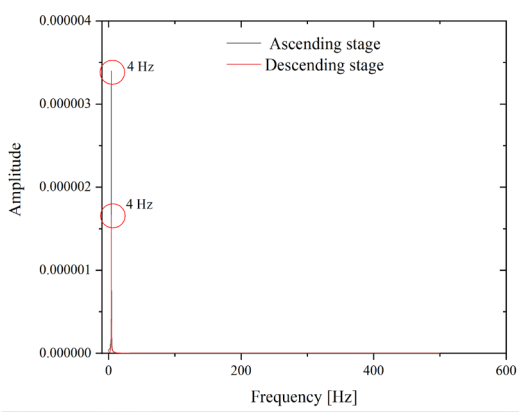

Fig. 6. *Extracted frequency spectrum of the elevator traction system without the eccentric excitation*

Fig. 6 shows the frequency spectrum of the elevator traction system obtained by Fourier transform of the time history of the longitudinal vibration during uniform motion in both ascending and descending processes without eccentric excitation. As shown in Fig. 6, the fundamental frequencies of the elevator traction system during uniform motion in both ascending and descending processes are 4 Hz.

3.2 Vibration Response with Eccentric Excitation

The eccentric excitation distance e is applied at the top of the rope and is expressed as:

$$e = 1 \times 10^{-4} \sin \omega_0 t \ \ [\mathrm{m}], \quad (27)$$

where ω_0 is the angular velocity of the lift machine and is closely related to the diameter d_0 of the traction wheel, the maximum hoisting speed v_m and the maximum acceleration a_m of the elevator traction system. In this paper, the angular velocity of the lift machine ω_0 is calculated by considering that the

distance travelled by the elevator per unit of time must equal that of the traction wheel and is estimated as follows:

$$\omega_0 = \frac{2l_T}{d_0 t_7}, \tag{28}$$

where l_T is the distance travelled by the elevator in a running cycle, and t_7 is the time period of a running cycle.

3.2.1 *Influence of the Running Direction*

In this subsection, the diameter of the traction wheel, the maximum hoisting speed and the maximum acceleration of the elevator traction system are chosen as d_0 = 0.4 m, v_m = 2.5 m/s, a_m = 0.5 m/s², and ω_0 = 3π. The time intervals of the seven stages are the same as those in Table 1 of Section 3.1. The time history of the longitudinal vibration of the elevator traction system in the process of ascending and descending is drawn in Fig. 7. It can be seen from Fig. 7 that the amplitude of the longitudinal vibration of the elevator traction system with external excitation gradually decreases during the ascending process and increases during the descending process, which is consistent to the response for the elevator traction system without eccentric excitation in Section 3.1. Nevertheless, the time histories shown in Fig. 7 for the elevator with eccentric excitation are quite different from those in Fig. 5 for the elevator without eccentric excitation.

To facilitate explain the reason for the difference, frequency spectra for the time history in Fig. 7 are extracted and plotted in Fig. 8. As shown in Fig. 8, the leading frequency is 1.5 Hz, which is the frequency of the lift machine. Furthermore, the fundamental frequency 4 Hz of the elevator traction system is also captured. The spectrum analysis indicates that the vibration response of the elevator with eccentric excitation is governed by eccentric excitation.

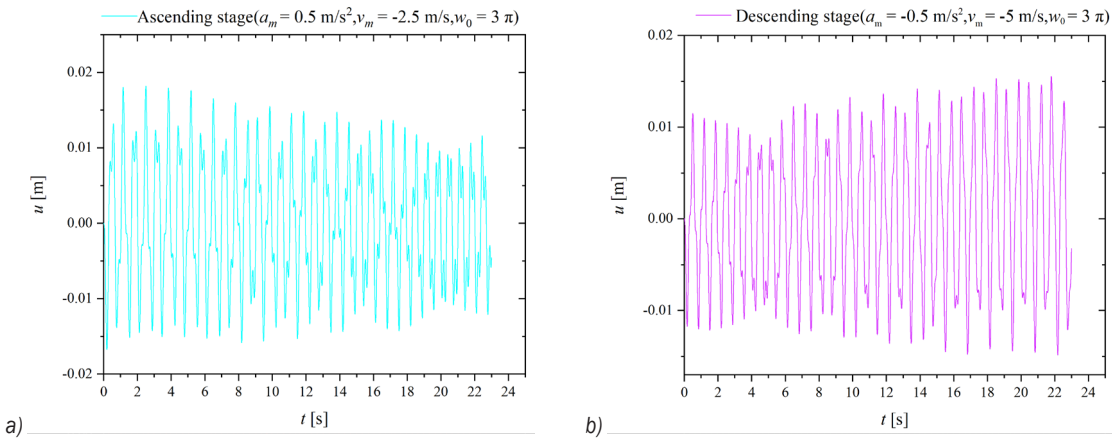

Fig. 7. *The time history of the elevator traction system caused by external eccentric excitation.; a) ascending stage, and b) descending stage*

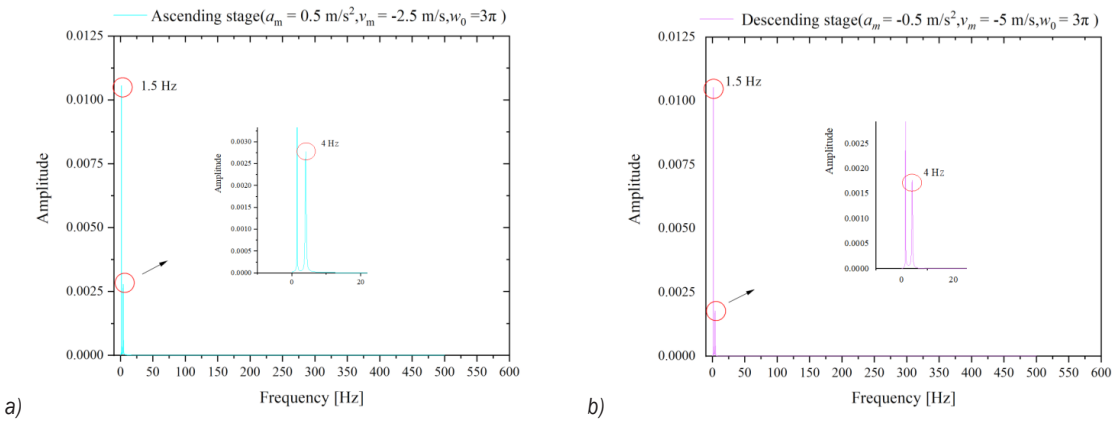

Fig. 8. *Extracted frequency spectrum of the elevator traction system with eccentric excitation; a) ascending stage, and b) descending stage*

3.2.2 Influence of the Acceleration of the Elevator

To clarify the influence of the acceleration of the elevator traction system on its vibration performance, the following three cases in which the elevator goes down are investigated:

Case I v_m = -3.75 m/s, a_m = -0.75 m/s2, $\omega_0 = 9/2\pi$;
Case II v_m = -5.0 m/s, a_m = -1.0 m/s2, $\omega_0 = 6\pi$;
Case III v_m = -7.5 m/s, a_m = -1.5 m/s2, $\omega_0 = 9\pi$.

Fig. 9 demonstrates the influence of the acceleration on the time history of the descending elevator traction system. It can be seen the vibration amplitude of the elevator traction system increases for all three cases during the descending process. Furthermore, the vibration amplitudes of the elevator for Case II are less than those for Case III but greater than those for Case I. In other words, the greater the values of vm and am, the larger the vibration amplitude of the elevator. However, Fig. 9c also shows that the amplitude of the elevator increases significantly at t = 13 s. Such a response indicates that the resonance occurs in the elevator traction system, as the frequency of the eccentric excitation of the traction machine is close to the fundamental frequency of the elevator traction system. Therefore, in order to prevent the occurrence of resonance and the maximum values of acceleration and deceleration should not exceed 1.5 m/s².

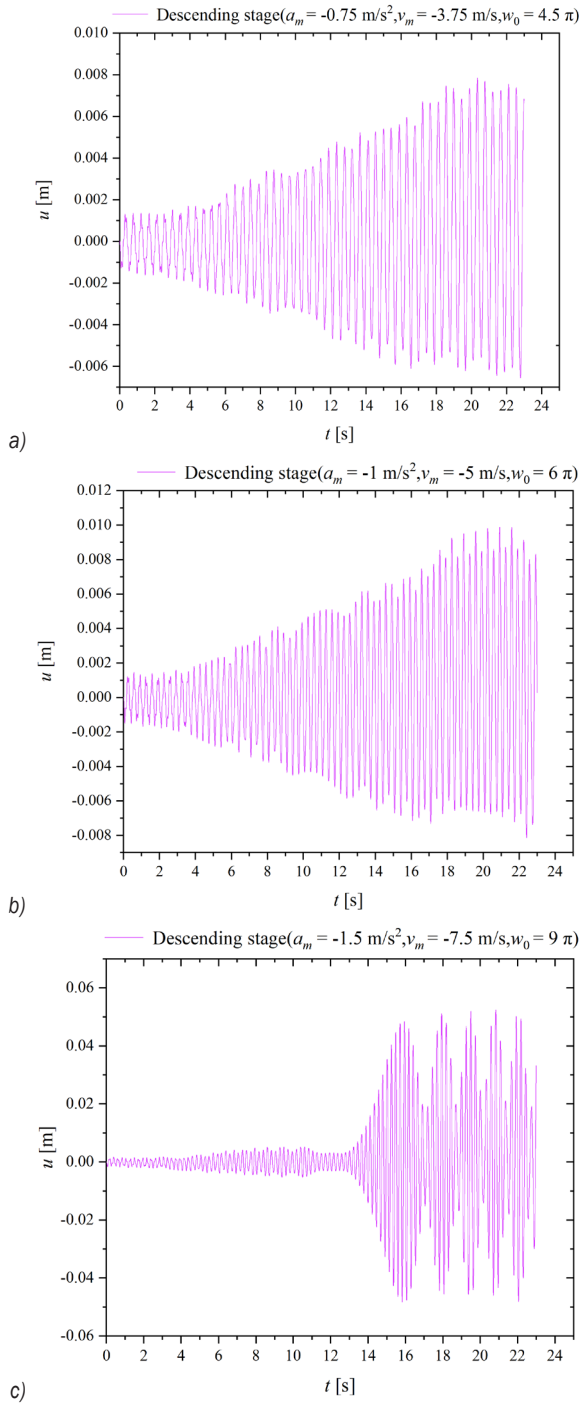

Fig. 9. *The influence of the acceleration on the time history of the descending elevator traction system; a) a_m = -0.75 m/s², b) a_m = -1 m/s², and c) a_m = -1.5 m/s²*

4 CONCLUSIONS

In this paper, the longitudinal vibration of the time-varying elevator traction system is studied by means of theoretical analysis and numerical simulation. The equation of motion and the corresponding boundary condition of the time-varying elevator traction system with and without external interference is derived based on the Hamiltonian principle and is solved by employing Galerkin's weighted residual method to take into consideration the boundary condition. As an application of the proposed analytical approach, the force vibration of the elevator traction system induced by the eccentric excitation of the traction wheel is analysed. Depending on the running status of the elevator, a mathematical formula is proposed to estimate the angular velocity of the traction wheel. A MATLAB program is developed to obtain the numerical solutions of the elevator traction system under different running statuses. The following conclusions can be drawn:

1. During the ascending stage, the equivalent stiffness of the elevator traction system increases with the decreasing length of the wire rope, resulting in a decrease in the vibration amplitude

and vibration frequency. The situation is reversed during the descending stage.

2. As far as the structural parameters of the elevator are determined, the vibration response of the elevator traction system is determined by its running state. In particular, the greater the running acceleration of the elevator, the larger the angular velocity of the traction wheel, and the higher the vibration amplitude and frequency of the elevator traction system.
3. When the acceleration reaches am = 1.5 m/s², the frequency of eccentric excitation of the traction machine is close to the fundamental frequency of the elevator traction system, which leads to the resonance of the elevator traction system. Therefore, in order to prevent the occurrence of resonance, the maximum value of acceleration and deceleration should not exceed 1.5 m/s².

In practical engineering applications, elevators are installed within buildings, so the vibration of elevators is affected by the vibration of buildings. Further experimental and theoretical studies can be conducted on the coupled vibration between the elevators and the buildings subjected to wind loads and earthquakes, which may provide a reference for seismic design of elevator traction system.

5 ACKNOWLEDGEMENTS

This work is supported by the Guangdong Natural Science Foundation (No. 2021A1515012037).

6 REFERENCES

[1] Cortés, P., Muñuzuri, J., Vázquez-Ledesma, L.A. (2021). Double deck elevator group control systems using evolutionary algorithms: Interfloor and lunchpeak traffic analysis. *Computers & Industrial Engineering*, vol. 155, art. ID 107190, **DOI:10.1016/j.cie.2021.107190**.

[2] Zhu, W.D., Teppo, L.J. (2003). Design and analysis of a scaled model of a high-rise, high-speed elevator. *Journal of Sound and Vibration*, vol. 264, no. 3, p. 707-731, **DOI:10.1016/S0022-460X(02)01218-X**.

[3] Meng, F., Chen, Y., Du, M., Gong, X. (2016). Study on effect of inter-wire contact on mechanical performance of wire rope strand based on semi-analytical method. *International Journal of Mechanical Sciences*, vol. 115-116, p. 416-427, **DOI:10.1016/j.ijmecsci.2016.07.012**.

[4] Zhang, J., Wang, D.G., Zhang, D.K., Ge, S.R, Wang, D.A. (2017). Dynamic torsional characteristics of mine hoisting rope and its internal spiral components. *Tribology International*, vol. 109, p. 182-191, **DOI:10.1016/j.triboint.2016.12.037**.

[5] Xiang, L., Wang, H.Y., Chen, Y., Guan, Y.J., Wang, Y.L., Dai, L.H. (2015). Modeling of multi-strand wire ropes subjected to axial tension and torsion loads. *International Journal of Solids and Structures*, vol. 58, p. 233-246, DOI:10.1016/j.ijsolstr.2015.01.007.

[6] Xiang, L., Wang, H.Y., Chen, Y., Guan, Y.J., Dai, L.H. (2017). Elastic-plastic modeling of metallic strands and wire ropes under axial tension and torsion loads. *International Journal of Solids and Structures*, vol. 129, p. 103-118, **DOI:10.1016/j.ijsolstr.2017.09.008**.

[7] Foti, F., de Luca di Roseto A. (2016). Analytical and finite element modelling of the elastic-plastic behaviour of metallic strands under axial-torsional loads. *International Journal of Mechanical Sciences*, vol. 115-116, p. 202-214, **DOI:10.1016/j.ijmecsci.2016.06.016**.

[8] Stanova, E., Fedorko, G., Kmet, S., Molnar, V., Fabian, M. (2015). Finite element analysis of spiral strands with different shapes subjected to axial loads. *Advances in Engineering Software*, vol. 83, p. 45-58, **DOI:10.1016/j.advengsoft.2015.01.004**.

[9] Wang, J.J., Cao, G.H., Zhu, Z.C., Wang, Y.D., Peng, W.H. (2015). Lateral response of cable-guided hoisting system with time-varying length: Theoretical model and dynamics simulation verification. *Proceedings of the Institution of Mechanical Engineers, Part C: Journal of Mechanical Engineering Science*, vol. 229, no. 16, p. 2908-2920, **DOI:10.1177/0954406214566032**.

[10] Peng, Q.F., Jiang, A.H., Yuan, H., Huang, G.J., He, S., Li, S.Q. (2020). Study on theoretical model and test method of vertical vibration of elevator traction system. *Mathematical Problems in Engineering*, vol. 2020, art. ID 851802, **DOI:10.1155/2020/8518024**.

[11] Xu, P., Peng, Q.F., Jin, F.S., Xue, J.H., Yuan, H. (2023). Theoretical and experimental study on tension-torsion coupling vibration for time-varying elevator traction system. *Acta Mechanica Solida Sinica*, vol. 36, p. 899-913, **DOI:10.1007/s10338-023-00429-5**.

[12] Zhang, R.J., Yang, W.W., Wang, X.W. (2014). The reliability analysis of horizontal vibration of elevator based on multi-state fuzzy Bayesian network. *Jordan Journal of Mechanical and Industrial Engineering*, vol. 8, no. 1, p. 43-49.

[13] Wang, J., Pi, Y., Krstic, M. (2018). Balancing and suppression of oscillations of tension and cage in dual-cable mining elevators. *Automatica*, vol. 98, p. 223-238, **DOI:10.1016/j.automatica.2018.09.027**.

[14] Trąbka, A. (2014). Dynamics of telescopic cranes with flexible structural components. *International Journal of Mechanical Sciences*, vol. 88, p. 162-174, **DOI:10.1016/j.ijmecsci.2014.07.009**.

[15] Zhang,Y., Zhang, Q., Peng, Y.X., Wang, C., Chang, X.D., Chen, G.A. (2022). Tribological behavior of octadecylamine functionalized graphene oxide modified oil for wire rope in mine hoist. *Wear*, p. 494-495, art. ID 204273, **DOI:10.1016/j.wear.2022.204273**.

[16] Bao, J.H., Zhang, P., Zhu, C.M. (2014). Transverse vibration of flexible hoisting rope with time-varying length. *Journal of Mechanical Science and Technology*, vol. 28, p. 457-466, **DOI:10.1007/s12206-013-1110-y**.

[17] Kaczmarczyk, S., Ostachowicz, W. (2003). Transient vibration phenomena in deep mine hoisting cables. Part 2: Numerical simulation of the dynamic response. *Journal of Sound and*

Vibration, vol. 262, no. 2, p. 245-289, **DOI:10.1016/S0022-460X(02)01148-3**.

[18] Zhang, R.J., Wang, C., Zhang, Q., Liu, J. (2019). Response analysis of non-linear compound random vibration of a high-speed elevator. *Journal of Mechanical Science and Technology*, vol. 33, p. 51-63, **DOI:10.1007/s12206-018-1206-5**.

[19] Cao, S.X., Zhang, R.J., Zhang, S.H., Qiao, S., Cong, D.S., Dong, M.X. (2019). Roller-rail parameters on the transverse vibration characteristics of super-high-speed elevators. *Transactions of the Canadian Society for Mechanical Engineering*, vol. 43, no. 4, p. 535-543, **DOI:10.1139/tcsme-2018-0083**.

[20] Zhang, R.J., Wang, C., Zhang, Q. (2018). Response analysis of the composite random vibration of a high-speed elevator considering the nonlinearity of guide shoe. *Journal of the Brazilian Society of Mechanical Sciences and Engineering*, vol. 40, art. ID 190, **DOI:10.1007/s40430-017-0936-0**.

[21] Gaiko, N.V., van Horssen, W.T. (2018). Resonances and vibrations in an elevator cable system due to boundary sway. *Journal of Sound and Vibration*, vol. 424, p. 272-292, **DOI:10.1016/j.jsv.2017.11.054**.

[22] Yang, D.H., Kim, K.Y., Kwak, M.K., Lee, S. (2017). Dynamic modeling and experiments on the coup-led vibrations of building and elevator ropes. *Journal of Sound and Vibration*, vol. 390, p. 164-191, **DOI:10.1016/j.jsv.2016.10.045**.

[23] Crespo, R.S., Kaczmarczyk, S., Picton, P., Su, H. (2018). Modelling and simulation of a stationary high-rise elevator system to predict the dynamic interactions between its components. *International Journal of Mechanical Sciences*, vol. 137, p. 24-45, **DOI:10.1016/j.ijmecsci.2018.01.011**.

[24] Nguyen, T.X., Miura, N., Sone, A. (2019). Analysis and control of vibration of ropes in a high-rise elevator under earthquake excitation. *Earthquake Engineering and Engineering Vibration*, vol. 18, p. 447-460, **DOI:10.1007/s11803-019-0514-9**.

[25] Knezevic, B.Z., Blanusa, B., Marcetic, D.P. (2017). A synergistic method for vibration suppression of an elevator mechatronic system. *Journal of Sound and Vibration*, vol. 406, p. 29-50, **DOI:10.1016/j.jsv.2017.06.006**.

[26] Zhang, Y.H., Agrawal, S.K., Hagedorn, P. (2005). Longitudinal vibration modelling and control of a flexible transporter system with arbitrarily varying cable lengths. *Journal of Vibration and Control*, vol. 11, no. 1, no. 3, p. 431-456, **DOI:10.1177/1077546305047988**.

[27] Qiu, L.M., Wang, Z., Zhang, S., Zhang, L., Chen, J.A. (2020). Vibration-related design parameter optimization method for high-speed elevator horizontal vibration reduction. *Shock and Vibration*, vol. 2020, art. ID 1269170, **DOI:10.1155/2020/1269170**.

[28] Yavuz, Ş., Malgaca, L., Karagülle, H. (2016). Analysis of active vibration control of multi-degree-of-freedom flexible systems by Newmark method. *Simulation Modelling Practice and Theory*, vol. 69, p. 136-148, **DOI:10.1016/j.simpat.2016.06.004**.